The Fate of Ethyl Pyruvate during Adsorption on Platinum Chirally Modified by Cinchonidine Studied by ATR−IR Spectroscopy†

Davide Ferri, Thomas Bürgi,‡ and Alfons Baiker*

Institute of Chemical and Bioengineering, Swiss Federal Institute of Technology, ETH Hönggerberg, CH - 8093 Zurich, Switzerland

Received: January 19, 2004; In Final Form: May 3, 2004

The behavior of ethyl pyruvate during adsorption on vapor deposited alumina-supported platinum films and on a commercial 5 wt % Pt/Al_2O_3 catalyst has been studied in the absence and presence of coadsorbed cinchonidine, which is usually applied as a chiral modifier in the platinum-catalyzed enantioselective hydrogenation of α-ketoesters. The in situ ATR−IR measurements, performed at room temperature using hydrogen-saturated CH_2Cl_2 as solvent, revealed that upon adsorption on the platinum some of the ethyl pyruvate decomposes leading to strongly adsorbed CO and other fragmentation products. The CO originating from decomposition of ethyl pyruvate reached approximately 14% of the amount of adsorbable CO on the free platinum surface and is proposed to be adsorbed preferentially on energetically favored sites such as edges and corners. The presence of cinchonidine (10^{-4} M) lead to a drastic decrease of the decomposition rate of ethyl pyruvate by a factor of about 60 under the conditions used. Competitive adsorption experiments of CO and cinchonidine in the presence of hydrogen indicated that cinchonidine can displace the adsorbed CO, confirming the strong anchoring of cinchonidine on the platinum surface, which is a prerequisite for its action as a chiral modifier. The findings of the adsorption studies provide a plausible explanation for the earlier made observation that the sequence of admission of α-ketoester, chiral modifier, and hydrogen affects the catalytic performance of platinum-catalyzed enantioselective hydrogenation. The decomposition is likely to occur also with other α-ketoesters and may have a bearing on the initial transient period, typically observed during hydrogenation of such compounds on cinchona-modified platinum catalysts.

Introduction

Among the various strategies used for the synthesis of chiral products, asymmetric catalysis has gained considerable attraction, boosted by the remarkable progress achieved with homogeneous catalysts.[1−3] Nevertheless, significant interest remains in heterogeneous asymmetric catalysts due to their intrinsic technical advantages concerning handling, separation, and regeneration. A number of heterogeneous catalysts have been reported that give very high enantioselection in asymmetric hydrogenation,[4,5] whereas catalysts for other reactions are still scarce.[6,7] A powerful method to impart chirality to an achiral active metal surface is the adsorption of a suitable chiral compound. The most prominent heterogeneous asymmetric catalysts that are based on this concept are cinchona-modified platinum for the hydrogenation of α-ketoesters,[8−10] alkaloid-modified palladium for the hydrogenation of functionalized olefins,[11−14] and tartaric acid modified nickel for the hydrogenation of β-ketoesters.[15−18] In the past decade considerable research effort has been expended aiming at a better fundamental understanding of the surface phenomena and mechanism involved in these enantioselective catalytic systems. Beside, the scope of reactions has been substantially extended. The gathered knowledge has been covered in several reviews.[19−24]

Although, most studies have been focused on the heterogeneous asymmetric hydrogenation of methyl and ethyl pyruvate on cinchona-modified platinum, originally reported by Orito,[8] several fundamental questions inherent for understanding the functioning of this fascinating catalytic system are still not resolved. A key for better understanding is the investigation of the adsorption and interaction of the chiral modifier and reactants, which has been the focus of several groups. Various techniques, including XPS,[25] LEED,[26] and NEXAFS[27,28] in the UHV environment, as well as Raman spectroscopy,[29] cyclic voltammetry,[30,31] RAIRS,[32−34] and ATR−IRS[35,36] for the solid−liquid interface have been applied to gain some insight in the adsorption behavior of cinchonidine and derivatives thereof on platinum. Methyl and ethyl pyruvate adsorption on platinum have been studied under UHV conditions by XPS and UPS,[37] XANES,[38] STM,[39] and NEXAFS,[28] and on Ni by RAIRS.[40,41] The decomposition path of methyl pyruvate on Ni(111) has been addressed by RAIRS in the temperature range 200−450 K.[42] The interaction between a chiral modifier and the α-ketoester reactant on the Pt surface has been in the focus of recent ATR−IR[43] and RAIR[44] studies.

Although, the adsorption studies of cinchonidine and alkyl pyruvates have brought important knowledge concerning the structure of adsorbed species, the coadsorption of these species with other species under reaction conditions is still unclear. Using ATR−IR spectroscopy different adsorption modes of cinchonidine have been identified on Pt/Al_2O_3 and the competitive adsorption of solvent decomposition products has been evidenced.[35,36] The influence of oxygen, hydrogen, and CO on the adsorption of cinchonidine on polycrystalline Pt has been in the focus of a recent RAIRS study.[34]

† Part of the special issue "Gerhard Ertl Festschrift".

* To whom correspondence should be addressed. Phone: +41 1 632 31 53. Fax: +41 1 632 11 63. E-mail: baiker@chem.ethz.ch.

‡ Present address: Université de Neuchâtel, Institut de Chimie, Av. de Bellevaux 51, CH − Neuchâtel, Switzerland.

10.1021/jp049737r CCC: $27.50
Published on Web 06/09/2004

The major aim of this study was to investigate how ethyl pyruvate adsorption is affected by the presence of cinchonidine. For this purpose we have studied in situ ethyl pyruvate adsorption and its coadsorption with cinchonidine in the presence of hydrogen on vapor-deposited alumina-supported platinum films and on a commercial 5 wt % Pt/Al_2O_3 catalyst. These investigations revealed that a substantial portion of ethyl pyruvate decomposes and results in the formation of adsorbed CO and other fragmentation products when exposed to platinum. This observation prompted us to extend our coadsorption studies to also include CO.

Experimental Section

Materials. Cinchonidine (Fluka, 98%), ethyl pyruvate (Fluka, ≥ 97%), trifluoroacetophenone (Fluka, ≥ 98%), and dichloromethane (Baker) solvent were used without further purification. H_2 (99.999 vol %) and N_2 (99.995 vol %) gases were supplied by PANGAS, whereas CO (0.5 vol % in Ar) was supplied by Sauerstoffwerke Lenzburg.

ATR−IR Spectroscopy. In situ ATR spectra were obtained using a Bruker IFS/66 spectrometer equipped with a liquid-nitrogen cooled HgCdTe photodetector by accumulating 200 scans at 4 cm^{-1} resolution. Trapezoidal 52 × 20 × 2 mm Ge internal reflection elements (IRE, 45°, Grazeby Specac) were coated on the large side with electron-beam physical-vapor-deposited Pt/Al_2O_3 films consisting of 100 nm Al_2O_3 and 1 nm Pt. Preparation and characterization of the films have been described elsewhere.[45] The coating materials (Pt wires, 99.99% and alumina pellets, 99.3%) were supplied by Unaxis Materials. After film deposition the IRE was fixed within the walls of a homemade stainless steel flow-through cell by means of viton O-rings. Cooling jackets mounted on the cell were used to keep the temperature at 283 K during experiments. The apparatus used for all experiments has been described in more detail elsewhere.[45] Solutions were saturated with the desired gas (N_2, H_2, or CO) and were allowed to flow through the cell by means of a microdosing pump (MDP-2, SWIP) at a speed of 1.7 mL/min. Before performing adsorption experiments, the metal surface was cleaned by flowing H_2-saturated CH_2Cl_2 on the Pt/Al_2O_3 film as described earlier.[35]

Experiments were also performed with a commercial 5 wt % Pt/Al_2O_3 catalyst (Engelhard 4759) and Al_2O_3 (Fluka, for chromatography). A suspension of the catalyst in H_2O (Merck) was stirred for about 2 h. The suspension was dropped onto a trapezoidal 52 × 20 × 2 mm ZnSe IRE. After drying in air at room temperature, the Pt/Al_2O_3 catalyst was gently washed with CH_2Cl_2 and then reduced under H_2 at 623 K for 2 h. At this point the coated IRE was mounted within the cell. Before adsorption experiments, the Pt/Al_2O_3 was treated with H_2-saturated CH_2Cl_2.

Results

The interaction of ethyl pyruvate with Pt/Al_2O_3 was studied under conditions close to the conditions used for hydrogenation. For this purpose CH_2Cl_2 solutions of ethyl pyruvate and cinchonidine were saturated with hydrogen.

Ethyl Pyruvate on Pt/Al_2O_3 Films. Figure 1a shows the ATR spectra of a 10^{-3} M solution of ethyl pyruvate on an H_2-cleaned Pt/Al_2O_3 thin film at 283 K. Strong signals develop at around 2000 and 1800 cm^{-1}, which shift to 2029 and 1810 cm^{-1} after 1 h on-stream. These signals are readily assigned to adsorbed CO (on top, CO_L, and in 2-fold coordination CO_B). The slightly dispersive line-shape of the CO_L signal is a characteristic of the thin Pt film as discussed in detail elsewhere.[46] Besides these bands, the weak signal at 1732 cm^{-1} visible on the lower frequency side of the CO_B signal is characteristic for the carbonyl stretching of dissolved ethyl pyruvate.[47] Further weak signals are observed at 1680, 1601, 1454, and 1345 cm^{-1}, the latter two being typical for CH_3 vibrations. A negative-going signal at ca. 1400 cm^{-1} is also evident. The presence of strong bands due to adsorbed CO, but also the weak CH_3 bands, clearly indicate that part of the ethyl pyruvate decomposes on the cleaned Pt surface, in agreement with previous data.[48] The intensity of the band associated with linear CO as a function of time shows a characteristic saturation-like behavior.

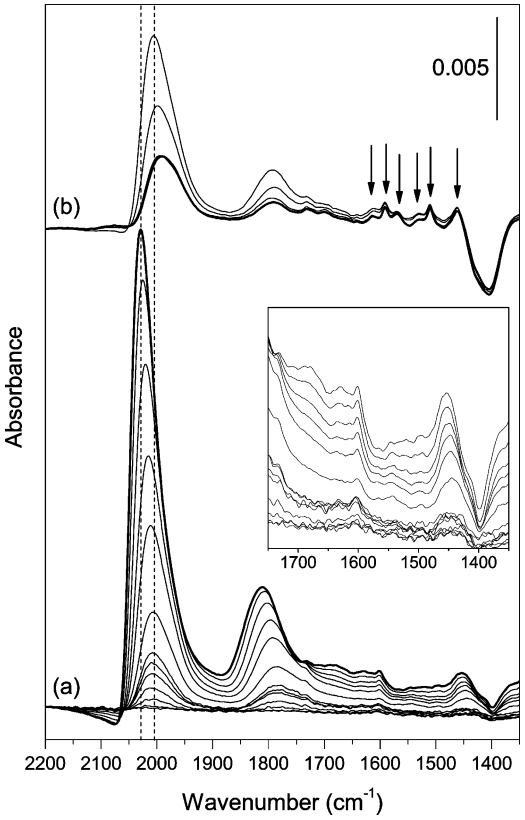

Figure 1. ATR spectra of a Pt/Al_2O_3 film at 283 K recorded during: (a) Ethyl pyruvate (10^{-3} M)/H_2 flow (∼ 60 min on stream) and (b) following cinchonidine (10^{-4} M)/ethyl pyruvate (10^{-3} M)/H_2 flow (∼ 30 min on stream). Arrows indicate the signals of adsorbed cinchonidine (see Ferri and Bürgi[35]). The first seven spectra in (a) were taken in rapid scan mode (at 9 scans/s scanning rate). The vertical dashed lines guide the eye through the frequency evolution of the CO signal from low to high coverage. The inset is an enlargement of the 1750−1350 cm^{-1} spectral region during step (a). Spectra have been taken at the following adsorption times: (a) 0.4, 0.7, 1, 1.5, 1.8, 2, 2.4, 4, 9, 14, 22, 36, 55, and (b) 62, 64, 76, and 88 min on stream.

When cinchonidine (10^{-4} M) was added to the ethyl pyruvate solution in the presence of hydrogen (Figure 1b) following the decomposition of ethyl pyruvate as shown in Figure 1a, the signal of adsorbed CO_L was significantly reduced in intensity and shifted to 1996 cm^{-1}. Simultaneously, the signals of adsorbed cinchonidine appeared at 1613, 1591, 1570, 1529, 1510, and 1462 cm^{-1} (arrows in Figure 1b). The strong negative signal at ca. 1400 cm^{-1} and a weak one at ∼ 1338 cm^{-1} were previously assigned to solvent decomposition products CH_2 and $C-CH_3$ (ethylidyne), respectively, which are displaced from the surface by cinchonidine.[35,36] The signals of adsorbed cinchonidine are assigned to three different surface species as discussed in detail before.[35,36] Briefly, species ***1*** (according to the nomenclature given by Ferri and Bürgi[35]) strongly coordinates to Pt through the quinoline π-system. In species ***2*** the

hydrogen attached to the carbon in α-position to the quinoline N is abstracted leading to a relatively strong C−Pt bond. Finally, species ***3*** is only weakly bound via the N lone pair.

Although H_2 is known to promote the displacement of CO from Pt,[49,50] the displacement of adsorbed CO observed in Figure 1b has to be attributed to cinchonidine. The process of CO removal by H_2 from Pt/Al_2O_3 films has been studied in detail.[45] Upon admission of hydrogen-saturated CH_2Cl_2 to a CO covered surface, the CO_L signal is red-shifted and its intensity is slightly increased before it starts depleting. This process is very slow, even for CO coverages far from saturation.[45] In contrast, CO is immediately removed when cinchonidine is introduced to the cell (Figure 1b). Adsorption−decomposition of ethyl pyruvate in the presence of H_2 followed by a flow of H_2-saturated solvent supports this conclusion. In fact, after interrupting the ethyl pyruvate feed and switching to H_2-saturated solvent, the CO_L was slowly red-shifted, increased in intensity, and then started to be attenuated. Note also that the CO_L signal at 1996 cm^{-1} in Figure 1b is located at a lower frequency than the initial CO_L signal in Figure 1a obtained upon contacting ethyl pyruvate with the Pt/Al_2O_3 film.

The extent of CO displacement depended on the concentration of the alkaloid in solution. Concentrations of 5×10^{-6}, 4×10^{-5}, and 10^{-4} M have been tested. Experiments were carried out by first exposing the Pt/Al_2O_3 film to ethyl pyruvate in the presence of H_2 for 1 h, which led to the formation of CO on the surface as described above (Figure 1). After that, a solution of ethyl pyruvate, hydrogen, and cinchonidine at different concentrations was flown over the sample. With the lowest cinchonidine concentration (5×10^{-6} M) the CO_L signal was not attenuated but did not increase further. At the higher cinchonidine concentrations the CO_L signal was significantly attenuated, the difference between 4×10^{-5} and 10^{-4} M being only minor.

Figure 2a depicts the spectrum of a chirally-modified Pt/Al_2O_3 film obtained by admitting a 10^{-4} M solution of cinchonidine in H_2-saturated CH_2Cl_2 as described earlier.[35] The spectrum shows the characteristic signals of adsorbed cinchonidine according to the three species mentioned above. When a solution of ethyl pyruvate and cinchonidine in H_2-saturated CH_2Cl_2 was admitted to such a Pt/Al_2O_3 film the signals due to CO at 2000 and 1796 cm^{-1} increased slowly and were rather weak, as can be seen in Figure 2b. Interestingly, when dissolved CO was admitted following the two previous steps, the CO_L and CO_B signals increased faster, as shown in Figure 2c. However, even after 1 h the intensity of the CO signal reached only about one-third of the value on a cleaned Pt/Al_2O_3 film.

Adsorption of CO and Cinchonidine. Figure 3 shows the maximum intensity of the CO_L signal as a function of time for the following experiments: (a) adsorption of CO from solution on the Pt/Al_2O_3 film, (b) exposure of the Pt/Al_2O_3 film to ethyl pyruvate (10^{-3} M) and hydrogen corresponding to the spectra shown in Figure 1a, and (c) exposure of the Pt/Al_2O_3 film to ethyl pyruvate (10^{-3} M), cinchonidine (10^{-4} M), and hydrogen after pre-exposing the film to cinchonidine corresponding to the spectra shown in Figure 2b. All three procedures lead to the adsorption of CO on Pt, though to a different extent. The spectra in Figure 4 correspond to the last point of each curve in Figure 3 (after ca. 60 min on stream). It is clear from the two figures that the development of CO proceeds with rather different rates for the three processes.

An approximate initial rate of CO formation can be determined from the CO_L signal for the three cases, assuming that one monolayer of CO (saturated layer) is obtained after about

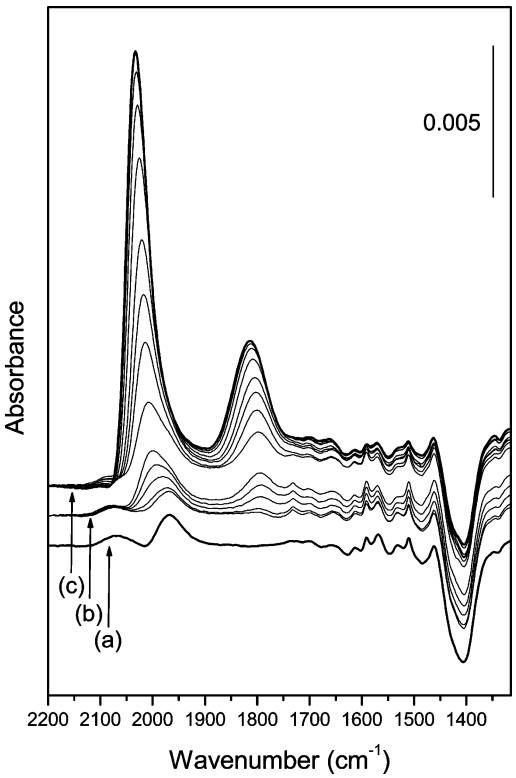

Figure 2. ATR spectra recorded during interaction of a cinchonidine-covered Pt/Al_2O_3 film with ethyl pyruvate at 283 K. Curve (a) is the last spectrum recorded during cinchonidine adsorption from a 10^{-4} M solution in H_2-saturated CH_2Cl_2. (b) Subsequent exposure of modified film to ethyl pyruvate, 10^{-3} M solution in H_2-saturated CH_2Cl_2 containing cinchonidine 10^{-4} M (80 min on stream). (c) Adsorption of CO from CH_2Cl_2 following steps (a) and (b) (60 min on stream). Spectra in (b) and (c) have been taken at the following adsorption times: (b) 0, 6, 12, 26, 46, and (c) 83, 86, 89, 91, 94, 104, 114, and 124 min on stream.

50 min of CO exposure (Figure 4a). This is not entirely correct since the CO_L signal slightly increases further by about 4% in the following 80 min. The estimate furthermore assumes that absorbance is proportional to coverage**,** which has been proven for low coverage on Pt single crystals.[51,52] The calculated initial rate of adsorption of CO on Pt is 11×10^{-4} monolayer/s, whereas the initial rate of CO build-up due to ethyl pyruvate decomposition in the absence and presence of cinchonidine is 6×10^{-4} and 0.1×10^{-4} monolayer/s, respectively. This shows that the decomposition of ethyl pyruvate affords CO at a rate that is approximately half of that achieved by adsorbing CO (0.5% in Ar) from CH_2Cl_2. More importantly, the presence of cinchonidine (10^{-4} M) leads to a decrease of the decomposition rate of ethyl pyruvate by a factor of 60.

CO is not only a decomposition product of ethyl pyruvate, it can also be used as probe molecule, by which the amount of available Pt surface sites can be estimated. Figure 5 depicts the evolution of the CO signal when adsorbing CO on Pt from CO-saturated solvent (a) until (close to) surface saturation and (b) by admitting a solution of cinchonidine (10^{-4} M) before saturation. As previously described,[45] CO shows the typical band shift and intensity increase as adsorption proceeds on the Pt/Al_2O_3 thin films. The CO_L signal exhibits a saturation-like curve as shown in Figure 5a. As demonstrated in Figure 1, part of the CO resulting from ethyl pyruvate decomposition is quickly removed by cinchonidine. Correspondingly, Figure 5b clearly shows the fast depletion of adsorbed CO upon adsorption of cinchonidine. The intensity of the remaining CO_L signal represents only about 16% of a saturated CO layer. The latter

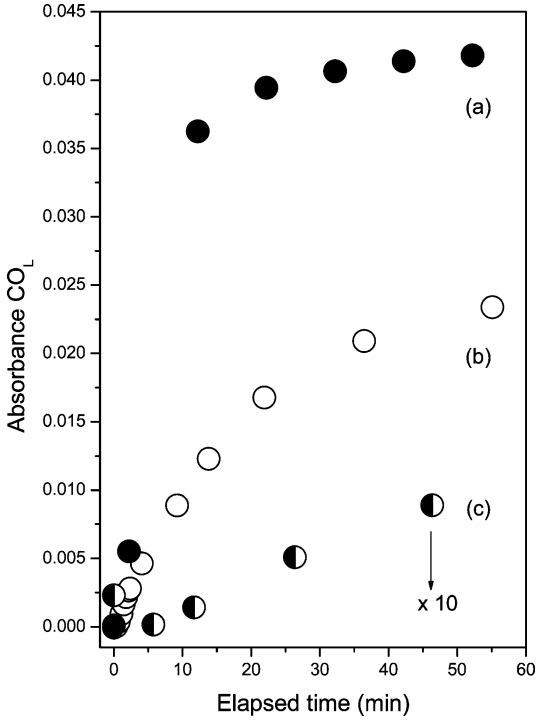

Figure 3. Maximum absorbance of the CO_L signal on Pt/Al_2O_3 as a function of time during exposure to: (a) CO (0.5% in Ar) dissolved in CH_2Cl_2, (b) ethyl pyruvate (10^{-3} M) in H_2-saturated CH_2Cl_2, and (c) ethyl pyruvate (10^{-3} M) and cinchonidine (10^{-4} M) in H_2-saturated CH_2Cl_2 on cinchonidine precovered Pt/Al_2O_3. Curves (b) and (c) correspond to spectra in Figs. 1a and 2b, respectively. The first data in (c) (time 0) corresponds to spectrum (a) in Figure 2. The values corresponding to experiment (c) are magnified 10 times for a better comparison.

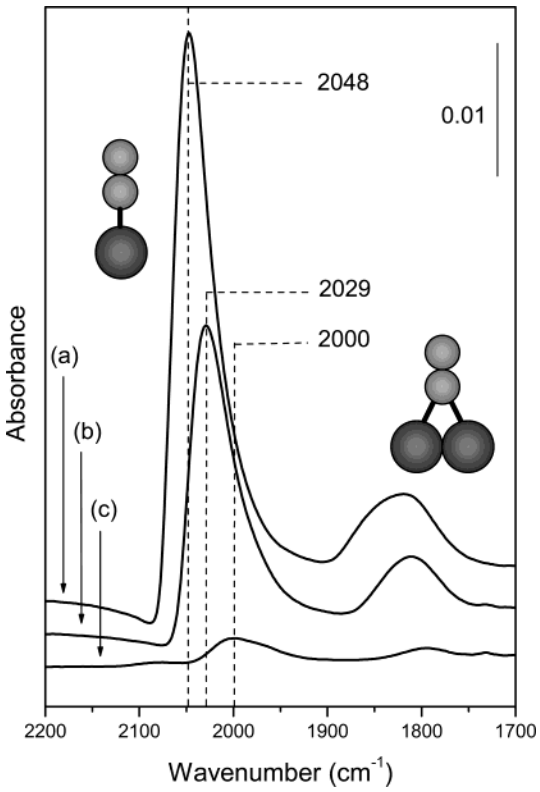

Figure 4. ATR spectra obtained after ca. 60 min on stream for the corresponding experiments shown in Figure 3.

was prepared by admitting CO in CH_2Cl_2 for about 150 min, at which time the CO signal remains approximately constant

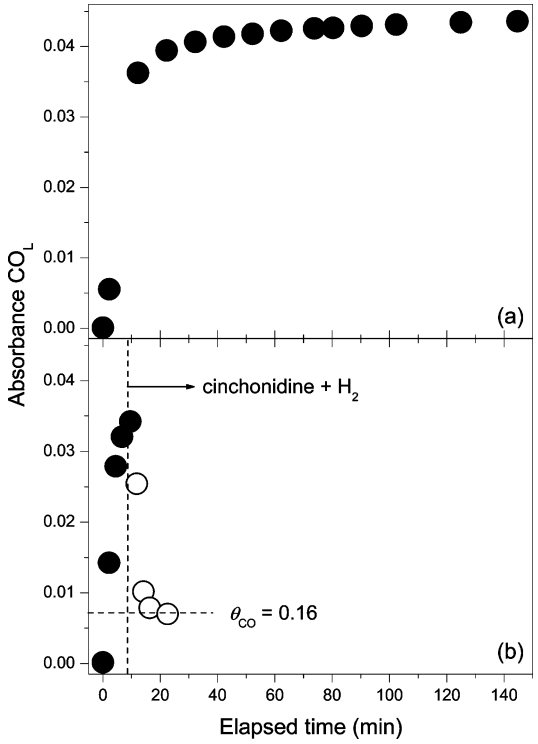

Figure 5. Maximum absorbance of the CO_L signal on Pt/Al_2O_3 as a function of time during exposure to (a) CO (0.5% in Ar) dissolved in CH_2Cl_2 (b) CO and then a solution of cinchonidine (10^{-4} M) in H_2-saturated CH_2Cl_2. The vertical line indicates the switching from CO to the cinchonidine solution.

(Figure 5a). It must be mentioned that the addition of cinchonidine and H_2 on a fully CO-covered Pt surface did not induce any change in the ATR spectra, indicating that no CO could be displaced by cinchonidine.

Adsorption of CO and Ethyl Pyruvate on Commercial Pt/Al_2O_3. Figure 6 shows ATR spectra of a preliminary study of CO and ethyl pyruvate adsorption from CH_2Cl_2 on commercial Pt/Al_2O_3 following H_2-cleaning of the catalyst. In Figure 6a the characteristic signals of adsorbed CO_L and CO_B can be easily distinguished at 2049 and 1818 cm^{-1}.

When ethyl pyruvate was contacted with the Pt/Al_2O_3 catalyst from a 10^{-3} M solution in H_2-saturated CH_2Cl_2, a CO_L signal was observed at 2029 cm^{-1} together with signals growing in at 1730, 1721, 1652, 1616, 1507, 1473, 1384, 1303, 1225, 1182, 1137, and 1010 cm^{-1} (Figure 6b). A strong, rather broad signal also developed at ca. 3100 cm^{-1}. Negative-going signals are also found at 3665, 1563, and 1422 cm^{-1}. Almost all signals were attenuated by the following flow of H_2-saturated solvent.

To assign qualitatively the signals observed in Figure 6b, ethyl pyruvate was also contacted with a commercial Al_2O_3 under the same experimental conditions used for the Pt/Al_2O_3 catalyst. Figure 6c shows that ethyl pyruvate adsorbs on Al_2O_3 and that signals emerge at 1734, 1716, 1645, ~ 1615, 1509, 1449, 1397, 1375, 1287, 1226, 1181, 1125, 1108, and 1015 cm^{-1}. The intensity of these signals was not affected by the following H_2-saturated solvent flow. The stronger intensity observed for the signals found on alumina with respect to those found on Pt/Al_2O_3 has to be attributed to the amount of powder deposited on the IRE, which was visibly higher in the case of Al_2O_3. It is however clear that the signals observed for ethyl pyruvate on Pt/Al_2O_3 correspond to those found for ethyl pyruvate on alumina, except for the adsorption of CO.

The stretching vibration of the carbonyl groups of neat and dissolved ethyl pyruvate shows a characteristic envelope with

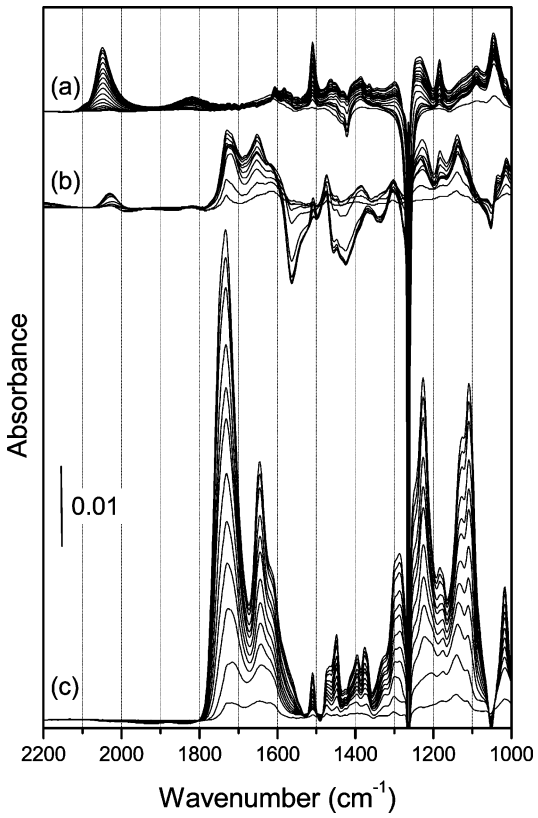

Figure 6. ATR spectra of commercial 5 wt % Pt/Al_2O_3 catalyst recorded during (a) adsorption of CO and (b) exposure to ethyl pyruvate (10^{-3} M) in H_2-saturated CH_2Cl_2. Ethyl pyruvate (10^{-3} M in H_2-saturated CH_2Cl_2) adsorbed on commercial Al_2O_3 is also shown for comparison (c). The sharp negative signal at 1264 cm^{-1} is uncompensated CH_2Cl_2 solvent. The overall time of adsorption is (a) 90, (b) 60, and (c) 80 min.

a maximum at 1731 cm^{-1}.[47] The ATR spectra in Figure 6b and 6c show a band at $\sim$ 1730 cm^{-1} with shoulders at 1720 and 1740 cm^{-1}. It is likely that ethyl pyruvate forms hydrogen bonds with surface hydroxyl groups, which leads to the observed negative band at 3665 cm^{-1}. The presence of a number of bands observed both on Pt/Al_2O_3 and Al_2O_3 indicates that on the support itself other processes may also occur, which involve ethyl pyruvate. Specifically, the bands observed at around 1620 cm^{-1} and the increasingly growing band at 1731 cm^{-1} may suggest that ethyl pyruvate is subject to side reactions on the Al_2O_3 support under the present experimental conditions.

Figure 7 shows the behavior of the CO signal when the α-ketoester is first contacted with the commercial Pt/Al_2O_3 catalyst followed by adsorption of CO from saturated solvent. More direct information on the adsorption process of ethyl pyruvate compared to that of CO can be gained. The signal of adsorbed CO grows in and reaches a maximum frequency of ca. 2030 cm^{-1} in the case of a flow of ethyl pyruvate, with a maximum intensity of about 0.002. After a short flow of H_2-saturated solvent (Figure 7b) CO is admitted to the surface from CO-saturated CH_2Cl_2. A stronger CO signal develops and reaches a maximum frequency of ca. 2060 cm^{-1} (Figure 7c). If the last point in Figure 7c is taken as the saturation point for CO on the Pt catalyst, the signal corresponding to CO formed from decomposition of ethyl pyruvate represents approximately 14% of the amount of adsorbable CO. Moreover, adsorbed CO originating from decomposition of ethyl pyruvate appears difficult to remove with H_2, as depicted in Figure 7b.

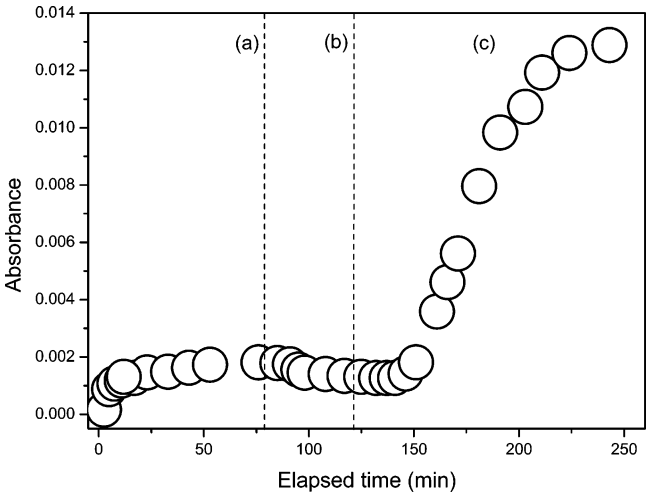

Figure 7. Maximum absorbance of the CO_L signal on the 5 wt % commercial Pt/Al_2O_3 catalyst as a function of time during exposure (a) to an ethyl pyruvate solution (10^{-3} M) in H_2-saturated CH_2Cl_2, (b) to H_2 dissolved in CH_2Cl_2, and (c) to CO (0.5% in Ar) dissolved in CH_2Cl_2.

Discussion

CO is the most significant species easily identified when contacting ethyl pyruvate with a cleaned Pt/Al_2O_3 film, specifically after treating the film with H_2-saturated solvent. Figure 1 shows that some other species develop on the film surface and are characterized by signals at 1680, 1601, 1454, and 1354 cm^{-1}. The accurate assignment of such signals to a defined species is rather difficult. However, the appearance of the signals is very likely related to the decomposition of ethyl pyruvate. It is reasonable to assume that the adsorption of CO from dissolved CO and from ethyl pyruvate decomposition follows different mechanisms. The decomposition route to afford CO must have some intermediates, which further evolve into CO.[53] McBreen et al.[40] reported that methyl pyruvate adsorbs on Ni(111) in a *cis*-conformation up to around 200 K but observed a breaking of the C−C bond connecting the carbonyl and the ester group already at 250 K.[41,42] A signal at ca. 1680 cm^{-1} was assigned to $CH_3OC{=}O$, methoxycarbonyl, and indirect evidence was given for adsorption of $CH_3C{=}O$, acetyl, whose methyl group could absorb higher than 1300 cm^{-1}. It seems therefore reasonable to assign the observed signals in Figure 1a to similar fragments. In any case the assignment of the broad signal at 1680 cm^{-1} and that at 1600 cm^{-1} to carbonyl-containing species is likely. The signal at 1345 cm^{-1} is associated with the umbrella mode of a methyl group. It should however be kept in mind that the decomposition route of pyruvates on Ni and Pt may still be different,[42] given the fact that the adsorption of organic fragments can differ significantly on the two metals.

It is also known that polymers can be formed on the Pt surface from condensation between methyl pyruvate molecules as observed in a vacuum on Pt(111) by STM.[39] The investigation however also clearly showed that H_2 suppresses the polymerization process. The spectra shown in Figure 1 and analysis of the frequency region at around 3000 cm^{-1} (not shown) do not give any evidence for such a process, which would be characterized by increasing signals due to C−H stretching vibrations. On the other hand, Figure 6 clearly shows that on a commercial catalyst other processes than adsorption and/or decomposition of ethyl pyruvate can occur, which we attribute to the presence of the alumina support. One important difference between the two films on the IRE, evaporated and commercial Pt/Al_2O_3, lies in the fact that in the former the contribution to

the spectroscopic data due to the metal is higher than in the latter, where the alumina support largely dominates. In fact, the signals observed in Figure 6 cannot be found in the spectra shown in Figure 1.

The inspection of Figure 2 leads to the important observation that ethyl pyruvate decomposition is suppressed or significantly hampered by the coadsorption of cinchonidine, whereas it is still possible to adsorb CO. This indicates that the decomposition of ethyl pyruvate to yield CO requires an accessible ensemble of Pt surface atoms that is larger than the ensemble needed to adsorb one CO molecule (one or two Pt atoms).

The amount of CO adsorbed in step (c) in Figure 2 can be viewed as a measure for the free Pt surface on the cinchonidine-covered surface. Assuming a maximum absorbance of 0.04 corresponding to a surface fully covered by CO and that absorbance is proportional to coverage, the absorbance of 0.0145 would correspond to 36% accessible surface in the presence of ethyl pyruvate and cinchonidine. This indicates that under the present experimental conditions cinchonidine adsorption on Pt does not afford an entirely covered chiral metal surface. That cinchonidine does not afford a compact film is also in good agreement with the results obtained by RAIRS[34] and cyclic voltammetry.[30,31] Attard et al.[30] found a value of 50% free surface for dihydrocinchonidine on Pt/graphite catalysts. Bakos et al.[31] determined by cyclic voltammetry of modified polycrystalline Pt that at most 50% of the Pt is covered by cinchonidine. It should however be noted that the electrochemical conditions are rather far from those used here.

The observation discussed above that ethyl pyruvate decomposition requires an ensemble of Pt surface atoms and that on a cinchonidine-covered surface such ensembles are rare has very likely consequences for practical application of the Pt/cinchonidine catalytic system. It has, namely, been found that the sequence of admission of cinchonidine modifier and reactant has a significant influence on the outcome of the reaction.[54] In view of the above-discussed findings one can easily imagine that a Pt catalyst exposed to the reactant before the modifier will be covered by decomposition products to a much larger extent than a catalyst, which is exposed first to the modifier. Figures 2 and 3, which show considerable slower ethyl pyruvate decomposition on cinchonidine-covered Pt support this statement.

The present data point out how the decomposition of ethyl pyruvate on both a model film and a commercial catalyst leads to CO formation. In order for the enantioselective hydrogenation of the α-ketoester to take place the chiral modifier has to adsorb onto the metal surface. The presence of a solvent and hydrogen involves a competition between the alkaloid and the solvent decomposition products at the metal-solution interface.[35,36] Moreover, cinchonidine does not adsorb on unreduced Pt surfaces, so that it must compete with surface impurities coming from the exposure of reactive platinum to air and from the possible decomposition of the solvent on the metal. Hydrogen favors cinchonidine adsorption by reducing the platinum surface and exposing cleaned Pt atoms, which behave as adsorption sites for the alkaloid.[34,35] The results presented above yield information on the relative adsorption strength of cinchonidine and CO on Pt under hydrogenation conditions. It is known that cinchonidine has to compete with CO for adsorption,[34] which is considered a poison for Pt. Figure 1 clearly shows that cinchonidine can displace the strongly adsorbed CO from the surface underlining its robust anchoring on the Pt, a property that is considered essential for functioning as modifier.[20] Figure 5 shows that this displacement takes place very fast. Cinchonidine can also easily remove CO from the metal surface at CO coverage close to saturation but not at saturation, where linear and bridged CO covers the cleaned Pt surface. This process is independent from the origin of CO, that is, regardless if coming from the direct adsorption of CO from solution or from ethyl pyruvate decomposition as Figures 1 and 5 indicate.

The peculiar shape (and intensity) of the CO signal in Figure 2a deserves a special mention. The two unusually high and low signals at 2080 and 1970 cm^{-1} are obtained when contacting cinchonidine with Pt.[35] Note that the small amount of CO observed in Figure 2a is present even without contacting the surface with ethyl pyruvate. A reasonable explanation for the origin of CO upon adsorption of cinchonidine on Pt is that cinchonidine displaces carbonaceous fragments from the metal surface, which decompose to CO. The displacement of CHx-like fragments by the chiral modifier is evoked by the negative signal at ca. 1400 cm^{-1} (Figure 1b and Figure 2a). The unusual CO signal has been observed before.[36] Different feasible reasons may be at the origin of this effect. The Pt sample used here is certainly heterogeneous; that is, different Pt sites are present. The existence of special $Pt-Al_2O_3$ boundary sites on the same type of Pt film has already been evidenced.[55] The observed bimodal CO signal could then arise, when CO is only adsorbed at special Pt sites. For example, edge or boundary sites (low frequency CO band) and at partially oxidized Pt sites (high frequency CO band) but not on the terraces, which usually provide the largest amount of sites for CO adsorption, corresponding to ν(CO) vibrations higher than 2000 cm^{-1}. A weak band at 2090 cm^{-1} has been reported for CO adsorbed on colloidal Pt/ poly(vinylpyrrolidone) from CO-saturated CH_2Cl_2, that is, under conditions close to those used in this study, and was assigned to CO adsorbed on oxidized Pt.[56] We tentatively assign the signal observed at 2080 cm^{-1} in Figure 2 to CO adsorbed on partially oxidized Pt sites, whereas the band at 1970 cm^{-1} is attributed to CO adsorbed at $Pt-Al_2O_3$ boundary sites, according to our previous findings.[55] The observation that this effect is found in the presence of cinchonidine could therefore be an indication that the relative adsorption strengths of CO and cinchonidine on Pt depend on the structure and electronic property of the metal site. The lack of the "normal" CO signal in Figure 2a therefore indicates that cinchonidine, relative to CO, is more strongly bound to terraces, whereas CO is more strongly bound to edge sites and partially oxidized Pt sites. This explanation supports previous experimental findings. First of all, IR spectra of adsorbed cinchonidine and quinoline indicate that at least part of the strongly anchored cinchonidine is bound via the quinoline π-system. Such an adsorption requires a considerable ensemble of Pt atoms and is therefore preferred on flat Pt surfaces. On the other hand, it has been found by electrochemical measurements that cinchonidine desorbs on oxidized Pt[31] and that adsorption is hindered when the Pt surface is contacted with oxygen before cinchonidine adsorption.[34]

Alternately a different coupling between adsorbed CO molecules in the presence and absence of cinchonidine could also be a feasible explanation for the origin of the bands observed at 2080 and 1970 cm^{-1}. Figure 1b shows that the frequency of CO_L observed in the presence of cinchonidine is slightly lower than that found at the early stages of CO adsorption originating from ethyl pyruvate decomposition on Pt (Figure 1a). Figures 2a and 2b show that independent CO species can be found on the Pt evaporated films: the CO present when adsorbing cinchonidine on Pt, characterized by the frequencies of 2080 and 1970 cm^{-1}, and the one building up on Pt after cinchonidine adsorption from EP decomposition or

CO adsorption. The latter CO leads to a signal above 1970 cm^{-1}. The shoulder of the main CO signal observed in Figure 2c at around 1970 cm^{-1} indicates that the CO adsorbed at the corresponding sites is still present and not affected by the further adsorption of CO. This observation favors the view that several CO bands are associated with distinct sites as discussed above rather than different vibrational coupling within the CO layer in the presence and absence of cinchonidine.

The behavior of the CO_L signal in Figure 1 further strengthens this conclusion. This signal is not only attenuated but also shifted toward a lower frequency upon adsorption of cinchonidine (and hydrogen). This low frequency is not observed at the early stages of CO adsorption in Figure 1a. After about 30 min under a stream of the cinchonidine solution the signal is found at 1996 cm^{-1}, again a relatively low frequency for linearly adsorbed CO. As stated above the signal may originate from CO adsorbed at sites that are not accessible for a relatively large molecule as cinchonidine. Figure 1 would suggest that upon adsorption of cinchonidine linear CO is removed from Pt terraces or large domains of Pt atoms. Alternatively, the remaining CO observed in Figure 1b could be assigned to individual CO species, which are usually characterized by a lower absorption frequency than CO in domains. However, the nature of the Pt/Al_2O_3 film[55] and the very low frequency observed for linear CO (below 2000 cm^{-1}) substantiate the adsorption of CO on different sites.

Figure 6 clearly demonstrates that ethyl pyruvate decomposes also on a commercial Pt/Al_2O_3 catalyst used in the enantioselective hydrogenation of α-ketoesters affording CO. Besides decomposition on Pt, Figure 6 also reveals side reactions on the metal oxide support. At present we are investigating the origin of the anomalous adsorption process observed in Figure 6 for ethyl pyruvate on Al_2O_3. The decomposition, and eventually also the side reactions as competing processes with respect to the actual hydrogenation and the concomitant build up of cinchonidine, are likely affecting the catalytic system even at high hydrogen pressure. Activated ketones seem to be prone to the decomposition. We should furthermore note that CO formation was observed also in the case of trifluoroacetophenone adsorption. Trifluoroacetophenone is currently hydrogenated on Pt/Al_2O_3 catalysts at low pressures.[57]

The decomposition process occurring on Pt leading to the observation of mainly CO has been followed on the Pt model film without any evident contribution from the Al_2O_3 support. Although some Al_2O_3 may be in contact with the solution, the most relevant interface in the Pt/Al_2O_3 model film is the Pt−solution interface. On the other hand, the spectra of the commercial Pt/Al_2O_3 catalyst, where the surface exposed to the solution is mainly Al_2O_3, show strong bands below 1700 cm^{-1} due to adsorption and/or reaction of ethyl pyruvate. Comparison of Figures 6b and 6c reveals that the Al_2O_3 is responsible for this observation, whereas the decomposition of ethyl pyruvate on Pt leads to CO. Figures 1 and 6 clearly demonstrate that distinct information can be obtained from both the model film and the catalytic material by means of attenuated total reflection infrared spectroscopy and that the contribution of the metal and metal oxide phases to the overall process can be separated to a certain extent.

The present in situ ATR−IR study of the adsorption behavior of ethyl pyruvate indicates that in the hydrogenation of alkyl pyruvates and probably also other α-ketoesters, a competing decomposition of the reactant leading to adsorbed CO and other fragmentation products can affect the catalytic performance, particularly at low hydrogen pressure. The decomposition of the reactant α-ketoester is mitigated in the presence of adsorbed cinchonidine and high hydrogen pressure. The spectroscopic findings provide a plausible explanation for the observation that the enantioselective hydrogenation of alkyl pyruvates over cinchona-modified platinum is affected by the sequence of admission of reactant and modifier to the reaction system.[54] The undesired side reactions leading to partial blocking of platinum surface sites can be suppressed by proper contacting of the platinum with reactant, modifier, and solvent.

The fragmentation of the α-ketoester may also have a bearing on the initial transient period observed during enantioselective hydrogenation.[58,59] Further in situ spectroscopic studies at hydrogen pressures typically used for hydrogenation will be necessary to finally assess the role of the reactant decomposition in the enantioselective hydrogenation of alkyl pyruvates.

Conclusions

The ATR infrared experiments show that ethyl pyruvate partly decomposes when contacted with Pt/Al_2O_3 films or commercial powder Pt/Al_2O_3 catalysts in hydrogen-saturated solvent. Besides the strong CO signals, weaker bands associated with other fragments can be observed on Pt. The observation of carbonyl vibrations suggests the presence of fragments such as methoxycarbonyl and acetyl. The modification of the Pt surface significantly affects the observed behavior. Cinchonidine adsorption is so strong that it can partly displace CO from the surface, a process that is fast. The peculiar shape of the CO signal at low coverage on a modified surface furthermore indicates that the CD adsorption strength with respect to CO is particularly strong on terraces. This is attributed to a particular adsorption mode of CD, which requires the interaction of the quinoline π-system with a relatively large ensemble of Pt surface atoms.

On unmodified Pt, CO signals due to adsorption of CO from solution or from ethyl pyruvate decomposition increase initially at a comparable rate. On modified Pt, however, the decomposition of ethyl pyruvate is considerably hindered, whereas CO from solution can still easily adsorb. This shows that the decomposition of ethyl pyruvate requires a considerable ensemble of free Pt surface sites. The findings may explain the strong dependence of the catalytic system on the order of contacting the catalyst with reactant and modifier, that is, modifier first or reactant first. It is furthermore very likely that the observed decomposition selectively poisons the Pt surface, which may affect the catalytic behavior and contribute to the initial transient period observed with these hydrogenation reactions.

Acknowledgments. The authors gratefully acknowledge the financial support from the Swiss National Science Foundation and ETH Zurich.

References and Notes

(1) Knowles, W. S. *Angew. Chem., Int. Ed.* **2002**, *41*, 1998.
(2) Noyori, R. *Angew. Chem., Int. Ed.* **2002**, *41*, 2008.
(3) Sharpless, K. B. *Angew. Chem., Int. Ed.* **2002**, *41*, 2024.
(4) Baiker, A.; Blaser, H. U. In *Handbook of Heterogeneous Catalysis*; Ertl, G., Knözinger, H., Weitkamp, J., Eds.; Wiley-VCH: Weinheim, 1997; Vol. 5, p 2422.
(5) Baiker, A. *Curr. Opin. Solid State & Mater. Sci.* **1998**, *3*, 86.
(6) Hutchings, G. J.; Willock, D. J. *Top. Catal.* **1998**, *5*, 177.
(7) Hutchings, G. J. *Chem. Commun.* **1999**, 301.
(8) Orito, Y.; Imai, S.; Niwa, S. *J. Chem. Soc. Jpn.* **1979**, 1118.
(9) Orito, Y.; Imai, S.; Niwa, S. *J. Chem. Soc. Jpn.* **1980**, 670.
(10) Orito, Y.; Imai, S.; Niwa, S. *J. Chem. Soc. Jpn.* **1982**, 137.
(11) Borszeky, K.; Mallat, T.; Baiker, A. *Catal. Lett.* **1996**, *41*, 199.
(12) Nitta, Y. *Top. Catal.* **2000**, *13*, 179.
(13) Huck, W. R.; Mallat, T.; Baiker, A. *J. Catal.* **2000**, *193*, 1.

(14) Tungler, A.; Fogassy, G. *J. Mol. Catal. A: Chem.* **2001**, *173*, 231.
(15) Izumi, Y. *Adv. Catal.* **1983**, *32*, 215.
(16) Webb, G.; Wells, P. B. *Catal. Today* **1992**, *12*, 319.
(17) Sugimura, T. *Catal. Surv. Jpn.* **1999**, *3*, 37.
(18) Osawa, T.; Harada, T.; Takayashu, O. *Topics Catal.* **2000**, *13*, 155.
(19) Blaser, H. U.; Jalett, H. P.; Müller, M.; Studer, M. *Catal. Today* **1997**, *37*, 441.
(20) Baiker, A. *J. Mol. Catal. A: Chem.* **1997**, *115*, 473.
(21) Baiker, A. *J. Mol. Catal. A: Chem.* **2000**, *163*, 205.
(22) Wells, P. B.; Simons, K. E.; Slipszenko, J. A.; Griffiths, S. P.; Ewing, D. F. *J. Mol. Catal. A: Chem.* **1999**, *146*, 159.
(23) von Arx, M.; Mallat, T.; Baiker, A. *Top. in Catal.* **2002**, *19*, 75.
(24) Studer, M.; Blaser, H. U.; Exner, C. *Adv. Synth. Catal.* **2003**, *345*, 45.
(25) Simons, K. E.; Meheux, P. A.; Griffiths, S. P.; Sutherlands, I. M.; Johnston, P.; Wells, P. B.; Carley, A. F.; Rajumon, M. K.; Roberts, M. W.; Ibbotson, A. *Recl. Trav. Chim. Pays-Bas* **1994**, *113*, 465.
(26) Carley, A. F.; Rajumon, M. K.; Roberts, M. W.; Wells, P. B. *J. Chem. Soc., Faraday Trans.* **1995**, *91*, 2167.
(27) Evans, T.; Woodhead, A. P.; Gutiérrez-Sosa, A.; Thornton, G.; Hall, T. J.; Davis, A. A.; Young, N. A.; Wells, P. B.; Oldman, R. J.; Plashkevych, O.; Vahtras, O.; Agren, H.; Carravetta, V. *Surf. Sci.* **1999**, *436*, L691.
(28) Bonello, J. M.; Sykes, E. C. H.; Lindsay, R.; Williams, F. J.; Santra, A. K.; Lambert, R. M. *Surf. Sci.* **2001**, *482*−*485*, 207.
(29) Chu, W.; LeBlanc, R. J.; Williams, C. T. *Catal. Comm.* **2002**, *3*, 547.
(30) Attard, G. A.; Gillies, J. E.; Harris, C. A.; Jenkins, D. J.; Johnston, P.; Price, M. A.; Watson, D. J.; Wells, P. B. *Appl. Catal., A: General* **2001**, *222*, 393.
(31) Bakos, I.; Szabo, S.; Bartok, M.; Kalman, E. *J. Electroanal. Chem.* **2002**, *532*, 113.
(32) Kubota, J.; Zaera, F. *J. Am. Chem. Soc.* **2001**, *123*, 11115.
(33) Kubota, J.; Ma, Z.; Zaera, F. *Langmuir* **2003**, *19*, 3371.
(34) Ma, Z.; Kubota, J.; Zaera, F. *J. Catal.* **2003**, *219*, 404.
(35) Ferri, D.; Bürgi, T. *J. Am. Chem. Soc.* **2001**, *123*, 12074.
(36) Ferri, D.; Bürgi, T.; Baiker, A. *Chem. Commun.* **2001**, 1172.
(37) Bürgi, T.; Atamny, F.; Schlögl, R.; Baiker, A. *J. Phys. Chem. B* **2000**, *104*, 5953.
(38) Bürgi, T.; Atamny, F.; Knop-Gericke, A.-H.; Hävecker, M.; Schedel-Niedrig, T.; Schlögl, R.; Baiker, A. *Catal. Lett.* **2000**, *66*, 109.
(39) Bonello, J. M.; Williams, F. J.; Santra, A. K.; Lambert, R. M. *J. Phys. Chem. B* **2000**, *104*, 9696.
(40) Castonguay, M.; Roy, J. R.; Rochefort, A.; McBreen, P. H. *J. Am. Chem. Soc.* **2000**, *122*, 518.
(41) Castonguay, M.; Roy, J. R.; Lavoie, S.; Adnot, A.; McBreen, P. H. *J. Am. Chem. Soc.* **2001**, *123*, 6429.
(42) Castonguay, M.; Roy, J. R.; Lavoie, S.; Laliberté, M. A.; McBreen, P. H. *J. Phys. Chem. B* **2004**, *108*, 4134.
(43) Bonalumi, N.; Bürgi, T.; Baiker, A. *J. Am. Chem. Soc.* **2003**, *125*, 13342.
(44) Lavoie, S.; Laliberté, M. A.; McBreen, P. H. *J. Am. Chem. Soc.* **2003**, *125*, 15756.
(45) Ferri, D.; Bürgi, T.; Baiker, A. *J. Phys. Chem. B* **2001**, *105*, 3187.
(46) Bürgi, T. *Phys. Chem. Chem. Phys.* **2001**, *3*, 2124.
(47) Ferri, D.; Bürgi, T.; Baiker, A. *J. Chem. Soc., Perkin Trans. 2* **2000**, 221.
(48) Minder, B.; Mallat, T.; Pickel, K. H.; Steiner, K.; Baiker, A. *Catal. Lett.* **1995**, *34*, 1.
(49) de Ménorval, L. C.; Chaqroune, A.; Coq, B.; Figueras, F. *J. Chem. Soc., Faraday Trans.* **1997**, *93*, 3715.
(50) Benvenutti, E. V.; Franken, L.; Moro, C. C. *Langmuir* **1999**, *15*, 8140.
(51) Shigeishi, R. A.; King, D. A. *Surf. Sci.* **1976**, *58*, 379.
(52) Crossley, A.; King, D. A. *Surf. Sci.* **1977**, *68*, 528.
(53) de Jesús, J. C.; Zaera, F. *Surf. Sci.* **1999**, *430*, 99.
(54) Margitfalvi, J. L.; Minder, B.; Talas, E.; Botz, L.; Baiker, A. *Stud. Surf. Sci. Catal.* **1993**, *75*, 2471.
(55) Ferri, D.; Bürgi, T.; Baiker, A. *Phys. Chem. Chem. Phys.* **2002**, *4*, 2667.
(56) de Caro, D.; Bradley, J. S. *Langmuir* **1998**, *14*, 245.
(57) von Arx, M.; Mallat, T.; Baiker, A. *Tetrahedron: Asymmetry* **2001**, *12*, 3089.
(58) Wang, J.; Sun, Y.; LeBlond, C.; Landau, R. N.; Blackmond, D. G. *J. Catal.* **1996**, *161*, 752.
(59) Mallat, T.; Bodnar, Z.; Minder, B.; Borszeky, K.; Baiker, A. *J. Catal.* **1997**, *168*, 183.